Staphylococcal Enterotoxin C promotes *Staphylococcus aureus* Infective Endocarditis Independent of Superantigen Activity

Kyle J. Kinney[1], Phuong M. Tran[1, 3], Katherine N. Gibson-Corley[2], Ana N. Forsythe[1], Katarina Kulhankova[1], Wilmara Salgado-Pabón[3*]

[1]Department of Microbiology and Immunology, University of Iowa Carver College of Medicine, Iowa City, Iowa, USA. [2]Department of Pathology, University of Iowa Carver College of Medicine, Iowa City, Iowa, USA. [3]Department of Pathobiological Sciences, University of Wisconsin-Madison, Madison, Wisconsin, USA. *corresponding author: wsalgado@wisc.edu

Abstract

The superantigen (SAg) staphylococcal enterotoxin C (SEC) is critical for *Staphylococcus aureus* infective endocarditis (SAIE) as tested in rabbits. Its hallmark function and most potent biological activity is hyperactivation of the adaptive immune system. Superantigenicity was proposed as a major underlying mechanism driving SAIE but was not directly tested. With the use of *S. aureus* MW2 expressing SEC toxoids, we show that superantigenicity does not contribute to vegetation growth, to the magnitude of myocardial inflammation or to acute kidney injury. In contrast, superantigenicity contributes to hepatocellular injury and overall systemic toxicity. Recent studies indicate that SAgs directly inhibit endothelial cell migration. We show that SEC inhibits production of serpin E1, crucial in cell migration and vascular repair. This may be central to SEC's role in SAIE. This study highlights the critical contribution of an alternative function of SAgs to SAIE and broadens our current understanding of these molecules.

Introduction

Staphylococcus aureus infective endocarditis (SAIE) is an acute and invasive infection of the cardiac endothelium characterized by the appearance of vegetative lesions (*1*). *S. aureus* is the leading cause of infective endocarditis in the developed world (IE) (*2-4*). The pathognomonic vegetations are a meshwork of bacterial aggregates and host factors such as fibrin, fibrinogen, platelets, and red-blood cells that form predominantly on heart valves (*5*). SAIE results in significant damage to cardiac structures, in particular the valves and myocardium, due to tissue toxicity and abscess formation (*6*). Once established, SAIE can lead to severe complications, most notably congestive heart failure, stroke, acute kidney injury, and septic shock (*4, 6, 7*). Treatment of SAIE is challenging, requiring prolonged antibiotic therapy or surgery to remove infected valves (*4, 6*). Even with treatment, SAIE has a high rate of recurrence and a 22-66% mortality rate (*2, 4*). Infections are frequently associated with methicillin-resistant *S. aureus* (MRSA) which complicate treatment and increase mortality (*8*). Furthermore, life-saving medical interventions (i.e. valve replacement, cardiac devices, and hemodialysis), an increasing population with underlying conditions (i.e. diabetes mellitus and immunosuppression), and advanced age also increase the risk of acquiring *S. aureus* infections (*2, 4*). As a result, the incidence of SAIE in the developed world has continued to increase (*4*). Unfortunately, the great advances in cardiovascular medicine achieved in the last decade have failed to improve SAIE outcomes. Thus, the mechanistic understanding of the pathophysiology of SAIE is not only of fundamental interest, particularly as it relates to bacterial factors critical for vegetation formation and development of complications, but also of utmost importance for development of effective intervention strategies.

Epidemiological studies demonstrated a strong association between SAIE and a select group of superantigen (SAg) genes, where 18-25% of SAIE strains encode *entC* (staphylococcal enterotoxin C; SEC), 9-20% encode *tstH* (toxic shock syndrome toxin; TSST1), and 58-90% encode the enterotoxin gene cluster (*egc*) (*9*). Consistent with these studies, SEC, TSST1, and the *egc* SAgs SEI, SE *like* (*l*)-M, SE*l*-O, and SE*l*-U all contribute to IE and metastatic infection in experimental IE (*10, 11*). However, the underlying mechanism by which SAgs contribute to SAIE pathogenesis remains speculative. Classically, SAgs are known for their potent T cell mitogenic activity resulting in dysregulated activation and cytokine production leading to inflammatory syndromes, and, in extreme cases, toxic shock (*12*). Superantigenicity results from toxin cross-linking of the Vβ chain of the T-cell receptor (TCR) to the major histocompatibility complex class II (MHC-II) receptor on antigen presenting cells (*12*). Of relevance to SAIE, endothelial cells also express MHC-II, thus functioning as conditional antigen presenting cells capable of cross-linking Vβ–TCR resulting in endothelium-mediated superantigenicity (*13*).

The dysregulated immune activation caused by SAgs distracts and diverts the immune system (*14*). It also promotes multiple etiologies including atopic dermatitis, pneumonia, extreme pyrexia, purpura fulminans, and toxic shock syndrome (*12*). The commonly accepted model of the role of SAgs in SAIE includes localized or systemic superantigenicity that causes dysregulation of the immune system preventing clearing of *S. aureus* from the infected heart endothelium. SAgs also cause capillary leak and hypotension that alters the hemodynamics of the vascular system (*12*). This alteration of blood flow may enhance vegetation formation. However, the requirement of superantigenicity in the pathogenesis and pathophysiology of SAIE has not been directly tested. In this study, we addressed the hypothesis that superantigenicity promotes SAIE and disease sequelae.

We used the rabbit model of native valve IE with the well-characterized MRSA strain MW2 (SEC^{+}) and MW2 stably expressing SEC toxoids (TCR or MHC-II/TCR inactivated) to provide evidence for the critical contribution of SEC but not superantigenicity to vegetation growth, to the magnitude of myocardial inflammation, and to injury to the renal and hepatic systems. We demonstrate that development of septic vegetations are a pre-requisite for embolic kidney injury and decreased renal function, while superantigenicity resulting from SAIE exacerbates embolic hepatocellular damage (even when exhibiting similar liver pathology) and exacerbates systemic toxicity. With the use of human aortic endothelial cells, we provide evidence that SEC selectively inhibits the pro-angiogenic factor serpin E1, demonstrating the ability of SEC to directly modify endothelial cell function in ways that can promote SAIE.

Results

Superantigenicity is not sufficient to promote vegetation formation

SAg activity is the most potent biological function of staphylococcal enterotoxins and causes lethal pathologies. To establish whether superantigenicity promotes development of SEC-mediated SAIE, we constructed a *S. aureus* strain expressing SEC with an inactive T-cell receptor (TCR) binding site (SEC_{N23A}). Asn^{23} is a highly-conserved, surface exposed residue located in a cleft between the O/B fold and β-grasp domain of SAgs (*15*). It forms hydrogen bonds with the backbone atoms of the complementarity-determining region (CDR) 2 of the Vβ-TCR (*16*). As such, Asn^{23} contact with the Vβ-TCR has one of the greatest energetic contributions of the complex. Mutations in this position, such as N23A or N23S, greatly destabilize the Vβ-TCR:SAg interaction with profound effects in SAg activity (*16*). SEC_{N23A} has no detectable binding to Vβ-TCR as measured by surface plasmon resonance, no proliferative T-

cell responses in thymidine-incorporation assays at concentrations up to 30 μg/ml (*16*), no lethality or signs of TSS in rabbits vaccinated subcutaneously with 25 μg three times every two weeks (*17*), and no lethality in rabbits after intravenous injection at 3,000 μg/kg (*18*). Due to its biological inactivation, SEC_{N23A} is excluded as a select agent toxin (*18*). Importantly, several vaccination studies have shown no disruption in toxin structure and in the antigenic nature of the protein (*17*, *19-21*).

MW2 (*S. aureus* SEC^{+}), the isogenic deletion strain MW2Δ*sec* (*S. aureus* SEC^{KO}), and MW2Δ*sec* complemented to produce SEC with an inactive TCR-binding site (*S. aureus* SEC_{N23A}) were tested in the rabbit model of native valve IE and sepsis (*10*). Rabbits were inoculated intravenously with 2-4 $x10^{7}$ total CFU after 2 hours of mechanical damage to the aortic valve and monitored for a period of 4 days. During that period, rabbits infected with *S. aureus* SEC^{KO} had a ~66% decrease in overall vegetation formation where 8/12 rabbits had no vegetations (Fig. 1A and B) and 4/12 had very small vegetations (sent to pathology) with an estimated weight of 5 – 15 mg (Fig. S1). In stark contrast, *S. aureus* SEC^{+} formed vegetations in nearly all rabbits (14/15). Of the 14 hearts containing vegetations, 6 were sent to pathology. In the rest (8/9), vegetation size ranged from 11 – 116 mg with most vegetations weighing >25 mg (Fig. 1A and B). Surprisingly, complementation with SEC_{N23A} restored vegetation formation to wild type levels (13/17), with vegetation sizes ranging from 12 – 103 mg (Fig. 1A and B). Vegetations formed by *S. aureus* SEC^{+} and *S. aureus* SEC_{N23A} also had comparable bacterial counts of $1x10^{7}$ – $4x10^{9}$ CFU (Fig. 1C). Of importance, *S. aureus* SEC^{+} and *S. aureus* SEC_{N23A} exhibited similar levels of SEC production in liquid culture (Fig. S2) and similar growth rates and red blood cell hemolysis (Fig. S2). Yet on average, serum IL-6 concentration was reduced in rabbits infected with *S. aureus* SEC_{N23A}, consistent with decreased systemic inflammation (Fig.

1D). These results indicate that SEC has SAg-independent activity that is important for the establishment and progression of vegetative lesions.

SEC mechanism in SAIE is independent of MHC class II interactions

To confirm the SAg-independent contribution of SEC to SAIE, we constructed a *S. aureus* strain expressing SEC with dual inactivation of the TCR- and MHC class II-binding sites ($SEC_{N23A/F44A/L45A}$). MHC-II is also expressed by non-hematopoietic cells such as epithelial cells and endothelial cells (*13*). Hence, we also could not exclude the possibility that the *in vivo* SEC_{N23A} interactions with MHC-II accounts for the observed phenotypes. SEC Phe^{44} and Leu^{45}, conserved among all enterotoxins, are located on a protruding hydrophobic loop that directly contacts MHC-II and forms strong electrostatic interactions with the α-chain (*22, 23*). Leu^{45} is the most extensively buried amino-acid residue in the SEC:MHC-II interface, but mutations in either residue (Phe^{44} or Leu^{45}) effectively inactivate SEC binding (*20-24*). F44S alone is 1000-fold less efficient in MHC-II binding resulting in a concomitant reduction of IL-2 in T-cell proliferation assays (*21, 25*). Simultaneous introduction of N23A/F44A/L45A in SEC does not affect protein production, with the complemented strains showing no deficiencies in growth rates and hemolytic activity (Fig. S2).

S. aureus $SEC_{N23A/F44A/L45A}$ was tested in the rabbit IE model as described above. As previously observed with *S. aureus* SEC_{N23A}, *S. aureus* $SEC_{N23A/F44A/L45A}$ produced vegetations at wildtype levels (12/17), with vegetations that ranged in size from 3 – 107 mg, most weighed >25 mg (Fig. 1A and B) and contained $5x10^7$ – $2x10^9$ CFU (Fig. 1C). Four of the 12 hearts containing vegetations were sent to pathology. The *S. aureus* $SEC_{N23A/F44A/L45A}$ strain on average also resulted in reduced serum IL-6 concentrations when compared to rabbits infected with *S. aureus*

138 SEC^{+} (Fig. 1D). Overall, infection with *S. aureus* strains producing toxoids formed vegetations
139 in 77% of the rabbits (26/34), compared to 93% (14/15) in rabbits infected with *S. aureus* SEC^{+}.
140 These results highlight the critical requirement of SEC in SAIE independent of superantigenicity
141 and MHC class II interactions.
142
143 **Superantigenicity does not drive myocardial inflammation in SAIE**
144 SAIE presents as a rapidly-growing and progressive vegetative lesion that results in the quick
145 destruction of valvular leaflets and extension of the infectious process into the myocardium and
146 adjacent structures (*5*). So far, the data supports a critical contribution of SEC but not
147 superantigenicity to vegetation growth on heart valves. We then asked whether SEC
148 superantigenicity promotes extension of the vegetative lesion into the surrounding tissue
149 changing the overall cardiac pathology. To address this, we performed histopathological analyses
150 on transverse sections of hearts containing vegetations. Rabbits infected with *S. aureus* SEC^{KO}
151 with no vegetations did not exhibit pathology at the end of experimentation (Fig. S1). Hence, we
152 processed all hearts of *S. aureus* SEC^{KO} infected rabbits with visible vegetations (mean size 2.7 ±
153 1 mm^2, n=4). Hearts from rabbits infected with *S. aureus* SEC^{+}, *S. aureus* SEC$_{N23A}$, or *S. aureus*
154 SEC$_{N23A/F44A/L45A}$ were selected randomly on the basis of presence of vegetations (mean size 6.6
155 ± 2 mm^2, n=15).
156 Consistent with histopathology of SAIE described in humans, *S. aureus* vegetations in
157 rabbits were composed of large aggregates of bacterial colonies interspersed in a fibrinous
158 meshwork of host factors and cell debris (Fig. S3-S5). However, the vegetative lesions were
159 heterogeneous across infection groups in presentation (location and size of bacterial clusters) and
160 in the magnitude of suppurative intracardial complications (myocardial inflammation and septic

coronary arterial emboli). In rabbits infected with *S. aureus* SEC^{+}(n=6), most vegetations were located on aortic valve cusps and valve leaflets, with large clusters of bacteria present on the leaflets and intermixed within the central core of the vegetation adjacent to the aorta. A few vegetations formed on the aortic wall were transmural (across the entire wall) and extended into the adjacent adipose tissue. Rabbits infected with *S. aureus*-producing SEC toxoids (SEC_{N23A} or $SEC_{N23A/F44A/L45A}$) exhibited very similar histologic presentation to each other and to those infected with *S. aureus* SEC^{+}, with a few exceptions. The endothelium adjacent to the vegetation of *S. aureus* producing SEC toxoids was rarely hypertrophied (plump) and the vegetation was not observed to form on valve leaflets. Strikingly, all of the small *S. aureus* SEC^{KO} vegetations formed on the aortic wall and extended into the adjacent adipose tissue (Fig. S1).

To directly address the contribution of SEC superantigenicity to myocardial inflammation, the magnitude of the inflammatory cell infiltrate was graded on a scale of 0-3 histologically (Fig. 2A). Most vegetative lesions presented with inflammation that was almost exclusively heterophilic (neutrophilic) adjacent to the vegetations (Fig. 2A). Foci of heterophils infiltrating the myocardium, cellular debris, and necrosis were also observed (Fig. 2A, insets). In the most severe cases (Grade 3), large and coalescing bands of heterophilic infiltrate surrounded the aortic ring (Fig. 2A). Vegetative lesions from *S. aureus* SEC^{+} consistently showed high grade myocardial inflammation that were indistinguishable histologically from those formed by *S. aureus* producing SEC toxoids (SEC_{N23A} or $SEC_{N23A/F44A/L45A}$) (Fig. 2B). Surprisingly, the *S. aureus* SEC^{KO} vegetations that formed on the aortic wall, albeit small, caused high grade inflammation adjacent to the vegetation. This is in stark contrast to the histopathology from rabbits infected with *S. aureus* SEC^{KO} with no vegetations, which was unremarkable (Fig. S1). Of interest, septic coronary arterial emboli (coronary arteries containing fibrin or bacterial

184 thrombi) with adjacent myocardial necrosis were observed in rabbits infected with *S. aureus*
185 SEC^{+} and SEC_{N23A} (Fig. 2C and E). Vegetations that penetrated deeper into the pericardium
186 causing epicardial lesions and saponification (necrosis) of epicardial fat were present in 5/15
187 rabbits infected with *S. aureus* SEC^{+} or *S. aureus* producing SEC toxoids (Fig. 2D and E).
188 Coronary emboli and epicardial lesions were observed in only 1/4 rabbits infected with *S. aureus*
189 SEC^{KO} (Fig. 2E). These observations indicate that intracardial complications, such as myocardial
190 inflammation, arise as a result of the presence of a vegetation and are independent of SEC
191 superantigenicity.
192
193 **SEC inhibits the pro-angiogenic factor serpin E1 in endothelial cells**
194 In acute IE, vegetative lesions develop rapidly with no evidence of repair (*26)*. The fact that SEC
195 promotes SAIE independently of superantigenicity suggests that it can directly target the
196 endothelium and modify its function. Re-endothelialization, driven by pro-angiogenic factors, is
197 essential for vascular endothelial repair (*27*). We hypothesized that SEC may dysregulate
198 angiogenesis as a mechanism to promote disease. To test this, immortalized human aortic
199 endothelial cells (iHAEC) were treated with 20 μg/ml of purified SEC and a protein array
200 utilized to measure changes in secreted angiogenesis-related proteins. Twenty-four soluble
201 factors produced by iHAEC were consistently detected in supernates (6 anti-angiogenic, 15 pro-
202 angiogenic, and 3 cytokines). A Log2 fold change of ± 1 was set as a threshold for relevant
203 changes (Fig. 3). None of the anti-angiogenic factors exhibited relevant changes from baseline.
204 Of the pro-angiogenic factors, serpin E1 [PAI-1 (plasminogen activator inhibitor-1)] exhibited on
205 average an 81% decrease (Log2 = -2.38) from baseline. The cytokines IL-1β, IL-8, and MCP-1
206 (monocyte chemoattractant protein-1) were not detected in amounts above threshold (Fig. 3).

The selective inhibition of the pro-angiogenic factor serpin E1 is consistent with the hypothesis that SEC inhibits angiogenesis in endothelial cells.

SEC contribution to vegetation formation is sufficient to promote high lethality

Cardiotoxicity and septic shock are complications associated with SAIE that frequently lead to higher mortality rates in humans (*4, 5, 28*). We had hypothesized that one of the mechanisms leading to high lethality in *S. aureus* SEC^{+} IE is vascular toxicity and multi-organ dysfunction resulting from superantigenicity (*10*). Yet, infection with either *S. aureus* SEC_{N23A} or *S. aureus* $SEC_{N23A/F44A/L45A}$ still led to high lethality, with ~50% of rabbits succumbing to infection during the experimental period (8/17 for SEC_{N23A} and 10/17 for $SEC_{N23A/F44A/L45A}$) compared to 73% of rabbits infected with *S. aureus* SEC^{+} (Fig. 4A). Rabbits infected with SEC-producing strains (wildtype or toxoid) consistently exhibited higher bacteremia ($>1x10^3$ CFU/ml) than those infected with *S. aureus* SEC^{KO} (Fig. 4B), which correlates with the presence of large septic vegetations. All strains tested presented with similar degrees of splenomegaly due to infection compared to uninfected controls (Fig. 4C). Thus, superantigenicity alone does not fully account for the high lethal outcomes associated with SEC production. Instead, SEC contribution to vegetation formation plays a prominent role in SAIE lethality.

Vegetation fragmentation and metastatic infection occur in one third of SAIE episodes and are associated with hemodynamic and embolic complications in multiple organ systems, including the vascular, nervous, pulmonary, gastrointestinal, renal, and hepatic systems (*4*). Septic embolization of cardiac vegetations increases mortality in patients with IE (*29*). In our previous studies, we noticed that rabbits consistently developed lesions in the liver and kidneys when infected with *S. aureus* wild type strains in the IE model (*30*). Hence, to further tease out

the contribution, if any, of superantigenicity to systemic complications associated with SAIE, we focused on the effect of SEC production to kidney and liver injury and function.

SEC causes renal impairment independent of superantigen-mediated toxicity

We had previously observed renal ischemia, infarction, and abscess formation associated with SEC production during SAIE in rabbits (*10*). It remained to be established if superantigenicity-mediated toxicity significantly contributed to acute kidney injury. To address this, all experimental rabbits were grossly assessed for kidney lesion pathology (n=61) on a scale from 0-3. The lesions presented as hemorrhagic, necrotic, or ischemic. In the most severe pathology (Grade 3), lesions were locally extensive, coalescing to diffuse, and extended across a large surface of the kidney (Fig. 5A, Table S3). Kidneys from *S. aureus* SEC^{+} infected rabbits presented with severe pathology (Grade 2-3) in 66% of the animals (Fig. 5B). Similar kidney pathology developed in 50% of rabbits infected with *S. aureus* producing SEC toxoids (8/17 for SEC_{N23A} and 9/17 for $SEC_{N23A/F44A/L45}$) (Fig. 5B). Overall, rabbits infected with SEC-producing strains (wildtype or toxoid) were more likely to develop severe kidney pathology compared to *S. aureus* SEC^{KO} infected rabbits (OR: 13.50, 95% CI: 1.931-150.2, $p = 0.0037$) (Fig. S6).

Consistent with kidney pathology, serum levels of blood urea nitrogen (BUN) and creatinine (biological markers of renal function) were significantly increased in rabbits infected with SEC-producing strains (Fig. 5C). BUN levels rose three-fold over pre-infection baseline in 89% of these rabbits (40/45) and creatinine rose two-fold in 44% (24/45). In stark contrast, few rabbits infected with *S. aureus* SEC^{KO} had dramatic fold changes over baseline, where only 17% (2/12) and 25% (3/12) exhibited similar increases in BUN and creatinine, respectively (Fig. 5C). These results provide evidence that acute kidney injury in experimental SAIE is likely due to

253 embolic disease (vegetation fragmentation and lodging in the kidneys) leading to decreased renal
254 function rather than kidney failure that is observed in toxic shock syndrome (*12*).
255
256 **Superantigenicity promotes hepatocellular injury and systemic toxicity**
257 SAIE can lead to acute liver injury through persistent systemic inflammation and hypoperfusion
258 (*31-33*), effects that can be secondary to superantigenicity. In our studies, liver pathology
259 presented as pale, streak-shaped lesions that where focal, multifocal, or coalescing (Fig. 6A).
260 Lesions were grossly scored on a scale from 0-3 (Table S3). In the most severe pathology (Grade
261 3), lesions presented as multifocal to coalescing, and extensive to diffuse throughout the surface.
262 Livers from *S. aureus* SEC^{+} infected rabbits presented with severe pathology (Grade 2-3) in 80%
263 of the animals (12/15; Fig. 6B). Similar liver pathology developed in ~70% of rabbits infected
264 with *S. aureus* producing SEC toxoids (9/17 for SEC_{N23A} and 13/16 for $SEC_{N23A/F44A/L45}$) (Fig.
265 5B). Overall, rabbits infected with SEC-producing strains (wildtype or toxoid) were more likely
266 to develop severe liver pathology compared to *S. aureus* SEC^{KO} infected rabbits (OR: 7.286,
267 95% CI: 1.806-26.91, $p = 0.0064$) (Fig. S6). Of note, in rabbits infected with *S. aureus* SEC^{KO},
268 severe liver pathology was largely observed only in rabbits that developed small aortic
269 vegetations (3/4 rabbits). These results indicate that SEC production and vegetation formation
270 are critical mediators of liver pathology, likely via the release of septic emboli based on gross
271 lesions.
272 To evaluate if superantigenicity, whether directly or indirectly, has an effect on liver
273 function, we measured serum levels of aspartate aminotransferase (AST) and alanine
274 aminotransferase (ALT; Fig. 6C). AST and ALT are biomarkers of hepatocellular damage.
275 Interestingly, rabbits infected with *S. aureus* SEC^{+} had significantly higher mean levels of AST

(236 U/L) and ALT (103 U/L) compared to those infected with *S. aureus* producing SEC toxoids or *S. aureus* SEC^{KO} (AST ≤ 73 U/L; ALT ≤ 76 U/L). Correspondingly, the ratio of AST to ALT was significantly higher in rabbits infected with *S. aureus* SEC^{+} (Fig. 6C). These rises in liver aminotransferase enzymes are consistent with what is observed in humans during acute liver injury and ischemic hepatitis (*32-33*). Of note, lactate dehydrogenase (LDH) was the only other enzyme, of those tested, differentially increased in rabbits infected with *S. aureus* SEC^{+} (Fig. 6C). LDH is found in almost every cell in the body, as such, is a non-specific biomarker of tissue damage. Therefore, superantigenicity increases overall tissue toxicity and hepatocellular injury, as reflected by increased levels of AST, ALT, and LDH.

Discussion

S. aureus SAgs are ubiquitous among human clinical isolates and implicated in both colonization and pathogenic mechanisms (*34*). Although their significance as virulence factors has been established, how SAgs specifically contribute to *S. aureus* pathogenesis has become a pressing question with the discovery of the multifunctionality of these toxins (*35-37).* Still, in SAg-mediated illnesses, superantigenicity is placed as a triggering event mediating or exacerbating pathological responses during *S. aureus* infection. Current evidence indicates that the SAgs SEC, TSST1 and select *egc* toxins play a novel and essential role in the etiology of SAIE by yet uncharacterized mechanisms (*10, 11*). It has been proposed that superantigenicity leading to hypotension and immune dysregulation allows bacterial immune evasion and persistence, while direct interaction with the heart endothelium promotes endothelium dysfunction and disease progression (*10, 11, 35*). With the use of *S. aureus* producing SEC inactivated in MHC-II and/or TCR binding, we provide evidence that superantigenicity is not the primary mechanism by which

SEC promotes vegetation formation, cardiac toxicity, and extracardiac complications such as such acute kidney injury. Our results are consistent with published studies noting that not all SAgs, such as the *egc* SAgs SEG and SE*l*-N, promote SAIE (*11*). SEG and SE*l*-N have comparable T cell mitogenic activity as SEA, SEB, and TSST1 (*38, 39*), indicating that superantigenic defects are not likely to account for their deficiency in promoting SAIE. It further highlights the critical contribution of SAgs, like SEC, in life-threatening pathologies by novel mechanisms that remain largely speculative or poorly understood at best.

The fact that SAgs promote SAIE development irrespective of their superantigenic activity indicates that their ability to target the endothelium and modify its function, as demonstrated for TSST1, may be an important mechanism contributing to disease development (*35*). TSST1 directly causes dysregulated activation of iHAECs and disrupts vascular integrity and re-endothelialization (*35*). Re-endothelialization is essential for vascular repair and wound healing and is dependent on angiogenic signals (*40*). Here we show that SEC selectively inhibits the pro-angiogenic factor serpin E1. Serpin E1, also known as plasminogen activator inhibitor type-1 (PAI-1), is particularly induced as part of the wound-repair program where it promotes endothelial cell migration towards fibronectin (*41*). The specific inhibition of serpin E1 in human umbilical vein endothelial cells (HUVECs) disrupts angiogenesis in *in vitro* cell migration and capillary network formation assays (*42*). Thus, SEC could promote IE if the injured endothelium is delayed from healing, exposing the sub-endothelial tissues and promoting deposition of fibrin, other pro-coagulants and *S. aureus*, ultimately contributing to initiation or spread of the vegetative lesion (*10, 34*).

Once established, SAIE is locally destructive, extending beyond the valve leaflets or valve cusps into perivalvular tissue, including the aortic wall, causing progressive myocardial

inflammation and abscess formation (*5*). Of great importance, the cardiac histopathology presentation of SAIE in rabbits is strikingly similar to that observed in humans. Myocardial inflammation is almost exclusively heterophilic causing aortic ring abscesses and necrosis in the most severe cases. Yet, myocardial inflammation resulting from *S. aureus* expressing SEC toxoids was not distinct from that caused by the wildtype strain. Therefore, while SEC is required for development of large septic vegetations, the data does not support a significant contribution of superantigenicity to the intracardiac heterophilic response that ensues following vegetation formation. It is unlikely that SEC solely drives this response as the atypical formation of small vegetations on the aortic wall in rabbits infected with *S. aureus* SEC^{KO} also leads to similar responses adjacent to the vegetation. *S. aureus* produces a multitude of secreted toxins and enzymes during invasive disease including the large family of cytolysins, proteases, and other SAgs that likely contribute to inflammation. Future studies will need to address the impact of any of these factors in SAIE cardiotoxicity.

SAIE has a high mortality rate owing to the high incidence of both intracardiac complications arising from the rapid local spread of the infection and the high incidence of embolization of septic vegetation fragments (*2, 4, 43*). Lodging of septic emboli within terminal blood vessels causes localized ischemia and infarction in multiple organ systems. In humans and in experimental rabbits, these complications can be manifested as myocardial infarction, kidney and/or liver injury, and strokes (*43*). Of these, kidney injury leading to acute renal insufficiency with progression to acute renal failure is tightly associated with SAIE severity, development of septic shock, and IE lethality (*7*). The role of SEC in kidney injury during SAIE has been demonstrated and it was proposed that SEC's role in inflammation, toxicity, or immune dysregulation was also required (*10*). Our studies rule out superantigenicity-mediated immune

345 dysregulation as the primary mechanism causing kidney injury. Rabbits infected with *S. aureus*
346 producing SEC toxoids develop severe kidney pathology coupled with significant decreases in
347 renal function. Furthermore, the type of lesions observed upon gross examination (hemorrhagic,
348 necrotic, or ischemic) are consistent with embolization of cardiac vegetations. Hence, the
349 contribution of SEC to kidney injury may be a consequence of its role in vegetation formation.
350 However, we have not ruled out a mechanism of renal deterioration arising as a direct effect of
351 SEC on the kidneys or its vasculature.

352 While the correlation between kidney function and poor prognosis in IE is well
353 established, literature on the effects of SAIE on liver injury is scarce (*4*). The liver has central
354 roles in clearing circulating bacteria and their toxins and is key in initiating or amplifying
355 inflammatory responses during systemic infections (*7*). Development of liver emboli has been
356 noted in patients with IE that develop septic shock, yet, not much more has been reported. In line
357 with published reports, we found that multifocal ischemic liver lesions were present grossly in
358 the great majority of rabbits infected with *S. aureus* SEC$^+$. As seen with the kidney, liver
359 pathology has a similar presentation in rabbits infected with strains producing wildtype SEC or
360 toxoids. Again, these results demonstrate a dependency on SEC for tissue injury that is
361 independent of superantigenicity. Hepatocellular injury as a result of extrahepatic bacterial
362 infection has been reported to be largely dependent on bacterial toxins (*7*). Indeed, AST and
363 ALT are increased >15 fold and >3 fold, respectively, in up to 40% of rabbits infected with *S.*
364 *aureus* SEC$^+$. In contrast to the kidneys, in the liver, superantigenicity significantly contributes to
365 hepatocellular injury. Increases in serum aminotransferases correlates with increases in IL-6 and
366 LDH in rabbits infected with *S. aureus* SEC$^+$ versus those infected with *S. aureus* expressing

SEC toxoids. Altogether, the data provides evidence for superantigenicity increasing hepatocellular injury during SAIE either directly or indirectly by increasing embolic events.

It is critical to recognize that while adaptive immune system activation is characteristic of staphylococcal SAgs, this is not their only biological function. Recently, the SAg SE*l*-X was found to inhibit neutrophil function via a sialic acid-binding motif uniquely present in this SAg (*37*). The SAgs TSST1, SEB, and SEC directly affect the function of endothelial/epithelial cells and adipocytes independent of superantigenicity (*35, 44, 45*). It was reported for TSST1 that activation of epithelial cells was caused by a dodecapeptide close to the base of the central α-helix of the molecule (*36*). The dodecapeptide sequence is found in all staphylococcal SAgs, yet its effects on non-hematopoietic cells is poorly characterized (*12, 36, 45*). The relevance of the SEC dodecapeptide in endothelial cell function and *S. aureus* diseases such as IE is currently being addressed.

In conclusion, we provide evidence that SEC is a multifunctional toxin critical to the pathogenesis and pathophysiology of SAIE. The superantigenicity independent effects of SEC are essential for the establishment of proliferative vegetations and systemic complications associated with disease progression. Overall, superantigenicity seems to exacerbate systemic inflammation and toxicity, with a significant contribution to hepatocellular injury. It now becomes possible to tease apart the localized SAg-host interactions triggering or exacerbating vegetation growth. It is also clear that SAgs do much more than previously anticipated or expected based on the current understanding of these molecules. Given the prevalence of SAgs among both methicillin-susceptible and resistant *S. aureus* strains, it becomes fundamental to understand the involvement of superantigenic-independent mechanisms in other invasive and life-threatening diseases.

Materials and methods

Bacterial strains and growth conditions. Staphylococcal strains were used from low-passage-number stocks. All staphylococcal strains were grown in Bacto™ Todd Hewitt (TH) (Becton Dickinson) broth at 37°C with aeration (225 rpm) unless otherwise noted. Strains and plasmids used in this study are listed in Table S1. Plasmids used for complementation were maintained using carbenicillin (100 μg/ml) in *E. coli* DH5α. For endocarditis experiments, strains were grown overnight, diluted, and washed in phosphate buffered saline (PBS - 2mM NaH_2PO_4, 5.7 mM Na_2HPO_4, 0.1 M NaCl, pH 7.4).

Construction of chromosomally complemented toxoid strains. SEC is a CDC designated select agent. As such, we are not allowed to use the wildtype copy of the gene in recombinant studies. For this reason, all PCR products generated in the making of the toxoid complement strains either included the permissible N23A SEC TCR mutation or was only a partial amplification of *sec* missing either the TCR or MHC-II domain. Each step of plasmid construction was verified by Sanger sequencing to contain the N23A TCR mutation. PCR amplification was performed using Phusion polymerase (New England Biolabs; NEB) unless otherwise noted. *S. aureus* expressing SEC_{N23A} or $SEC_{N23A/F44A/L45A}$ were made by markerless chromosomal complementation in MW2Δ*sec* (Table. S1) with the genes expressed under the control of the native promoter and terminator (*46*). The SEC_{N23A} gene sequence was created by amplifying two fragments from MW2 with primer sets pJB38xN23ApromF/promN23R and termN23F/pJB38xN23AtermR. The chromosomal complementation plasmid, pJB38-NWMN29-30, was digested with EcoRV and PCR products inserted by Gibson Assembly (NEB) as previously described, creating pKK29 (*47*). SEC_{N23} was amplified from pKK29 with the primer

set pUC19SECN23AptF/pUC19SECN23ApR and inserted into linearized pUC19, KpnI and EcoRI, by Gibson Assembly to create pKK33. The MHC-II binding site mutations were introduced into pKK33 by site-directed mutagenesis (QuickChange II, Agilent Technologies) using the primer set SECF44A/L45Afor/SECF44A/L45Arev, creating pKK39. The $SEC_{N23A/F44A/L45A}$ gene sequence was amplified from pKK39 with primer set pJB38xN23ApromF/ pJB38xN23AtermR and inserted into pJB38-NWMN29-30 as described above, creating pKK42. pKK29 and pKK42 were electroporated into *S. aureus* RN4220 and moved into MW2Δ*sec* by generalized transduction with ϕ11(*48*). *S. aureus* strains containing plasmid were selected for with chloramphenicol (20 µg/ml) at 30°C. Allelic exchange was performed as previously described (*46*), chromosomal insertions detected by PCR with primer set XNWMN2930F/XNWMN2930R, and verified by Sanger sequencing. Primers were purchased from Integrated DNA Technologies (Table S2).

Rabbit model of IE. The rabbit model of IE was performed as previously described with some modifications (*10*). 2-3 kg New Zealand White Rabbits were obtained from Bakkom Rabbitry (Red Wing, MN) and anesthetized with ketamine (dose range: 10-50 mg/kg) and xylazine (dose range: 2.5-10 mg/kg). Mechanical damage to the aortic valve was done by introducing a hard, plastic catheter via the left carotid artery, left to pulse against the valve for 2h, removed, and the incision closed. Rabbits were inoculated via the marginal ear vein with $2x10^7$-$4x10^7$ total CFU in PBS and monitored 4 times daily for a period of 4 days. For pain management, rabbits received buprenorphine (dose range: 0.01 – 0.05 mg/kg) twice daily. At the conclusion of each experiment, bacterial counts were obtained from heparinized blood (50 USP units/mL). Rabbits were euthanized with Euthasol (Virbac) and necropsies performed to assess overall health. Spleens were weighed and used as an infection control, kidney and liver gross

436 pathology was graded using gross lesion pathology scale (Table S3), aortic valves were exposed
437 to assess vegetation growth, and vegetations that formed were excised, weighed, and suspended
438 in PBS for CFU counts. A minimum of 4 rabbit hearts from each infection group were placed in
439 10% neutral buffered formalin and further processed by the Comparative Pathology Laboratory
440 at the University of Iowa for histopathological analyses. Vegetation weight and bacterial counts
441 cannot be obtained from hearts prepared for histology. All experiments were performed
442 according to established guidelines and the protocol approved by the University of Iowa
443 Institutional Animal Care and Use Committee (Protocol 6121907). All rabbit experimental data
444 is a result of at least 3 independent experiments per infection group.

445 **Histopathologic scoring.** Fixed tissues were routinely processed, cut at 5 μm, and
446 hematoxylin and eosin (HE) stained or Gram stained. Slides were reviewed and scored by a
447 board-certified veterinary pathologist.

448 **Serum analysis**. Rabbit serum was obtained from heparinized blood (50 USP units/mL)
449 collected before infection and at 48, 72, and 96 hpi. Blood was centrifuged at room temperature
450 at 5000 x g for 10 min. The collected supernatant was centrifuged for an additional 5 min, filter
451 sterilized using a 0.2 μm filter, and stored at -80°C for further analysis. Serum samples were sent
452 to the University of Iowa Diagnostic Laboratories and evaluated for the following serum
453 analytes: aspartate aminotransferase (AST; U/L), alanine aminotransferase (ALT; U/L), blood
454 urea nitrogen (BUN; mg/dl), creatinine (mg/dl), and lactate dehydrogenase (LDH; mg/dl).

455 **Rabbit IL-6 ELISA.** IL-6 was quantified from serum samples using the R&D Systems
456 DuoSet Rabbit IL-6 ELISA kit, according to manufacturer's instructions. Serum samples were
457 diluted 1:10 in reagent diluent prior to use. The optical density (O.D.) was determined using a
458 TECAN M200 plate reader (Tecan Group Ltd.) set to 450 nm with wavelength correction set to

459 540 nm. A standard curve was created by linear regression analysis of the IL-6 concentration
460 versus OD, log-transformed (GraphPad Prism 8).

461 **SEC purification.** SEC was purified from *S. aureus* strain FRI913 in its native form by
462 ethanol precipitation and thin-layer isoelectric focusing as previously described (*49*). Preparation
463 of SEC resulted in a single band by Coomassie blue stain. Toxin preparations were tested for
464 lipopolysaccharide (LPS) contamination with the ToxinSensor Chromogenic LAL Endotoxin
465 Assay following manufacturer's instructions (GenScript). SEC preparations had < 0.1ng of LPS
466 per 100 µg of toxin (< 0.02 ng of LPS per 20 µg of SEC).

467 **Human aortic endothelial cell culture.** Immortalized human aortic endothelial cells
468 (iHAECs) were cultured as previously described in Medium 200 with low-serum growth
469 supplement (both from Gibco Life Technologies) in 5% CO_2 at 37°C (*35*). All experiments were
470 conducted using iHAECs at 4-10 passages from a single clone.

471 **Proteome Profiler™ Human Angiogenesis Antibody array.** 96-well tissue culture
472 plates coated with 1% gelatin were seeded with 7,000 iHAECs/well and grown to confluence.
473 Fresh media containing purified SEC (20 µg/ml) was added and plates were incubated overnight
474 at 37°C with 5% CO_2. The supernatant was removed and stored at -80°C for further analysis.
475 The relative expression of 55 angiogenesis-related proteins was determined from the supernatant
476 using a Proteome Profiler™ Human Angiogenesis Antibody Array according to the
477 manufacturer's instructions (R&D Systems). 120 µL of supernates along with IRDye 800CW
478 Streptavidin (LI-COR, 1:2000 dilution) as a secondary antibody were used for this assay. The
479 fluorescent signal was detected using the LI-COR Odyssey CLx (84 µm resolution, auto
480 intensity 800 nm channel). Mean pixel density was calculated from duplicate spots on the
481 membrane and averaged using Image Studio Software (LI-COR). The log2 fold-changes over

media-only control were calculated for each detected protein. All treatments were matched to media only control. Data is a result of four biological replicas performed in duplicate.

Statistical analyses. The log-rank, Mantel Cox test was used for statistical significance of survival curves. Normality was assessed using the D'Agostino & Pearson test along with associated Q-Q plots for data distribution. For comparison across means log-transformed data was used and statistical significance was determined by using one-way analysis of variance (ANOVA) with the Holm-Sidak multiple comparison test for the following data sets: vegetation size, vegetation CFU, blood CFU, spleen size, BUN, creatinine, AST, ALT, LDH, and IL-6. Statistical significance for gross pathology data was determined using Fisher's exact test along with calculated odds ratios and 95% confidence intervals. Statistical significance of virulence factor production was determined by using the nonparametric Kruskal-Wallis test. $p \leq 0.05$ was considered statistically significant (GraphPad Prism 8).

References

1. V. G. Fowler, D. T. Durack, Infective endocarditis, *Curr. Opin. Cardiol.* **9,** 389-400 (1994).

2. V. G. Fowler, J. M. Miro, B. Hoen, C. H. Cabell, E. Abrutyn, E. Rubinstein, G. R. Corey, D. Spelman, S. F. Bradley, B. Barsic, P. A. Pappas, K. J. Anstrom, D. Wray, C. Q. Fortes, I. Anguera, E. Athan, P. Jones, J. T. M. Van Der Meer, T. S. J. Elliott, D. P. Levine, A. S. Bayer, Staphylococcus aureus endocarditis: A consequence of medical progress, *J. Am. Med. Assoc.* **293**, 3012–3021 (2005).

3. D. H. Bor, S. Woolhandler, R. Nardin, J. Brusch, D. U. Himmelstein, Infective Endocarditis in the U.S., 1998-2009: A Nationwide Study, *PLoS One*. **8**, e60033–e60033 (2013).

4. S. Y. C. Tong, J. S. Davis, E. Eichenberger, T. L. Holland, V. G. Fowler, Staphylococcus aureus infections: Epidemiology, pathophysiology, clinical manifestations, and management, *Clin. Microbiol. Rev.* **28**, 603–661 (2015).

5. G. Thiene, C. Basso, Pathology and pathogenesis of infective endocarditis in native heart valves, *Cardiovasc. Pathol.* **15**, 256–263 (2006).

6. M. L. F. Guerrero, J. J. G. López, A. Goyenechea, J. Fraile, M. De Górgolas, Endocarditis caused by staphylococcus aureus a reappraisal of the epidemiologic, clinical, and pathologic manifestations with analysis of factors determining outcome, *Medicine (Baltimore).* **88**, 1–22 (2009).

7. C. Olmos, I. Vilacosta, C. Fernández, J. López, C. Sarriá, C. Ferrera, A. Revilla, J. Silva, D. Vivas, I. González, J. San Román, Contemporary epidemiology and prognosis of septic shock in infective endocarditis, *Eur. Heart J.* **34**, 1999–2006 (2013).

8. E. Klein, D. L. Smith, R. Laxminarayan, Hospitalizations and deaths caused by methicillin-resistant Staphylococcus aureus, United States, 1999-2005, *Emerg. Infect. Dis.* **13**, 1840–1846 (2007).

9. J. J. C. Nienaber, B. K. Sharma Kuinkel, M. Clarke-Pearson, S. Lamlertthon, L. Park, T. H. Rude, S. Barriere, C. W. Woods, V. H. Chu, M. Marín, S. Bukovski, P. Garcia, G. R. Corey, T. Korman, T. Doco-Lecompte, D. R. Murdoch, L. B. Reller, V. G. Fowler, Methicillin-susceptible staphylococcus aureus endocarditis isolates Are associated with clonal complex 30 genotype and a distinct repertoire of enterotoxins and adhesins, *J. Infect. Dis.* **204**, 704–713 (2011).

10. W. Salgado-Pabón, L. Breshears, A. R. Spaulding, J. A. Merriman, C. S. Stach, A. R. Horswill, M. L. Peterson, P. M. Schlievert, E. J. Johnson, Ed. Superantigens are critical for Staphylococcus aureus infective endocarditis, sepsis, and acute kidney injury, *MBio.* **4**, e00494-13 (2013).

11. C. S. Stach, B. G. Vu, J. A. Merriman, A. Herrera, M. P. Cahill, P. M. Schlievert, W. Salgado-Pabón, Novel Tissue Level Effects of the Staphylococcus aureus Enterotoxin Gene Cluster Are Essential for Infective Endocarditis, *PLoS One.* **11**, e0154762–e0154762 (2016).

12. A. R. Spaulding, W. Salgado-Pabón, P. L. Kohler, A. R. Horswill, D. Y. M. Leung, P. M. Schlievert, Staphylococcal and streptococcal superantigen exotoxins, *Clin. Microbiol. Rev.* **26**, 422–447 (2013).

13. P. A. Brogan, V. Shah, N. Klein, M. J. Dillon, Vβ-restricted T cell adherence to endothelial cells: A mechanism for superantigen-dependent vascular injury, *Arthritis Rheum.* **50**, 589–597 (2004).

14. S. W. Tuffs, S. M. M. Haeryfar, J. K. McCormick, Manipulation of Innate and Adaptive Immunity by Staphylococcal Superantigens, *Pathog.* **7**, 53 (2018).

15. B. A. Fields, E. L. Malchiodi, H. Li, X. Ysern, C. V Stauffacher, P. M. Schlievert, K. Karjalainen, R. A. Mariuzza, Crystal structure of a T-cell receptor β-chain complexed with a superantigen, *Nature* **384**, 188–192 (1996).

16. L. Leder, A. Llera, P. M. Lavoie, M. I. Lebedeva, H. Li, R. P. Sékaly, G. A. Bohach, P. J. Gahr, P. M. Schlievert, K. Karjalainen, R. A. Mariuzza, A mutational analysis of the binding of staphylococcal enterotoxins B and C3 to the T cell receptor beta chain and major histocompatibility complex class II, *J. Exp. Med.* **187**, 823–833 (1998).

17. A. R. Spaulding, W. Salgado-Pabón, J. A. Merriman, C. S. Stach, Y. Ji, A. N. Gillman, M. L. Peterson, P. M. Schlievert, Vaccination Against Staphylococcus aureus Pneumonia, *J. Infect. Dis.* **209**, 1955–1962 (2013).

18. Nontoxic HHS toxins (Section 73.3(d)(2)), (Federal Register, CDC, 2016).

19. J. Y. Choi, S. Shin, N. Y. Kim, W. S. Son, T. J. Kang, D. H. Song, C. H. Yu, G. H. Hur, S. T. Jeong, Y. K. Shin, A novel staphylococcal enterotoxin B subunit vaccine candidate elicits protective immune response in a mouse model, *Toxicon* **131**, 68–77 (2017).

20. R. G. Ulrich, M. A. Olson, S. Bavari, Development of engineered vaccines effective against structurally related bacterial superantigens, *Vaccine*, **16**, 1857–1864, (1998).

21. M. A. Woody, T. Krakauer, B. G. Stiles, Staphylococcal enterotoxin B mutants (N23K and F44S): Biological effects and vaccine potential in a mouse model, *Vaccine* **15**, 133–139 (1997).

22. T. S. Jardetzky, J. H. Brown, J. C. Gorga, L. J. Stern, R. G. Urban, Y. Chi, C. Stauffacher, J. L. Strominger, D. C. Wiley, Three-dimensional structure of a human class II histocompatibility molecule complexed with superantigen, *Nature* **368**, 711–718 (1994).

23. R. Ulrich, S. Bavari, M. Olson, Staphylococcal enterotoxins A and B share a common structural motif for binding class II major histocompatibility complex molecules, *Nat. Struct. Biol.* **2**, 554–560 (1995).

24. M. A. Woody, T. Krakauer, R. G. Ulrich, B. G. Stiles, Differential Immune Responses to Staphylococcal Enterotoxin B Mutations in a Hydrophobic Loop Dominating the Interface with Major Histocompatibility Complex Class II Receptors, *J. Infect. Dis.* **177**, 1013–1022 (1998).

25. J. W. Kappler, A. Herman, J. Clements, P. Marrack, Mutations defining functional regions of the superantigen staphylococcal enterotoxin B, *J. Exp. Med.* **175**, 387–396 (1992).

26. C. N. Gentry, J. R. McDonald, Acute infective endocarditis, *Infect. Dis. Crit. Care* **23**, 271–283 (2007).

561 27. D. A. Chistiakov, A. N. Orekhov, Y. V Bobryshev, Endothelial Barrier and Its Abnormalities in Cardiovascular
562 Disease, *Front. Physiol.* **6**, 365 (2015).
563 28. C. K. Naber, Staphylococcus aureus Bacteremia: Epidemiology, Pathophysiology, and Management Strategies,
564 *Clin. Infect. Dis.* **48**, S231–S237 (2x009).
565 29. T. R. Wojda, K. Cornejo, A. Lin, A. Cipriano, S. Nanda, J. D. Amortegui, B. T. Wojda, S. P. Stawicki, Septic
566 Embolism A Potentially Devasting Complication of Infective Endocarditis, In: M.S. Firstenber (Ed.), Contemporary
567 Challenges in Endocarditis, *InTechOpen*. Chp. 8 (2016).
568 30. J. M. King, K. Kulhankova, C. S. Stach, B. G. Vu, W. Salgado-Pabón, Phenotypes and Virulence among
569 Staphylococcus aureus USA100, USA200, USA300, USA400, and USA600 Clonal Lineages, *mSphere* **1**, e00071-
570 16 (2016).
571 31. J. Yan, S. Li, S. Li, The role of the liver in sepsis, *Int. Rev. Immunol.* **33**, 498–510 (2014).
572 32. E. G. Giannini, R. Testa, V. Savarino, Liver enzyme alteration: a guide for clinicians, CMAJ. **172**, 367–379
573 (2005).
574 33. V. Fuhrmann, B. Jäger, A. Zubkova, A. Drolz, Hypoxic hepatitis – epidemiology, pathophysiology and clinical
575 management, *Wien. Klin. Wochenschr.* **122**, 129–139 (2010).
576 34. K. Werdan, S. Dietz, B. Löffler, S. Niemann, H. Bushnaq, R.-E. Silber, G. Peters, U. Müller-Werdan,
577 Mechanisms of infective endocarditis: pathogen–host interaction and risk states, *Nat. Rev. Cardiol.* **11**, 35–50
578 (2014).
579 35. K. Kulhankova, K. J. Kinney, J. M. Stach, F. A. Gourronc, I. M. Grumbach, A. J. Klingelhutz, W. Salgado-
580 Pabón, The Superantigen Toxic Shock Syndrome Toxin 1 Alters Human Aortic Endothelial Cell Function, *Infect.*
581 *Immun.* **86**, e00848-17 (2018).
582 36. A. J. Brosnahan, M. M. Schaefers, W. H. Amundson, M. J. Mantz, C. A. Squier, M. L. Peterson, P. M.
583 Schlievert, Novel toxic shock syndrome toxin-1 amino acids required for biological activity, *Biochemistry* **47**,
584 12995–13003 (2008).
585 37. S. W. Tuffs, D. B. A. James, J. Bestebroer, A. C. Richards, M. I. Goncheva, M. O'Shea, B. A. Wee, K. S. Seo,
586 P. M. Schlievert, A. Lengeling, J. A. van Strijp, V. J. Torres, J. R. Fitzgerald, The Staphylococcus aureus
587 superantigen SElX is a bifunctional toxin that inhibits neutrophil function, *PLoS Pathog.* **13** (2017).

588 38. 1. D. Grumann, S. S. Scharf, S. Holtfreter, C. Kohler, L. Steil, S. Engelmann, M. Hecker, U. Völker, B. M.
589 Bröker, Immune Cell Activation by Enterotoxin Gene Cluster (egc)-Encoded and Non- egc Superantigens from
590 Staphylococcus aureus, *J. Immunol.* **181**, 5054–5061 (2008).
591 39. D. S. Terman, A. Serier, O. Dauwalder, C. Badiou, A. Dutour, D. Thomas, V. Brun, J. Bienvenu, J. Etienne, F.
592 Vandenesch, G. Lina, Staphylococcal entertotoxins of the enterotoxin gene cluster (egcSEs) induce nitric oxide- and
593 cytokine dependent tumor cell apoptosis in a broad panel of human tumor cells, *Front. Cell. Infect. Microbiol.* **4**, 38
594 (2013).
595 40. D. A. Chistiakov, A. N. Orekhov, Y. V. Bobryshev, Endothelial barrier and its abnormalities in cardiovascular
596 disease, *Front. Physiol.* **6**, 365 (2015).
597 41. C. Isogai, W. E. Laug, H. Shimada, P. J. Declerck, M. F. Stins, D. L. Durden, A. Erdreich-Epstein, Y. A.
598 DeClerck, Plasminogen activator inhibitor-1 promotes angiogenesis by stimulating endothelial cell migration toward
599 fibronectin, *Cancer Res.* **61**, 5587–5594 (2001).
600 42. T. Masuda, N. Hattori, T. Senoo, S. Akita, N. Ishikawa, K. Fujitaka, Y. Haruta, H. Murai, N. Kohno, SK-216, an
601 Inhibitor of Plasminogen Activator Inhibitor-1, Limits Tumor Progression and Angiogenesis, *Mol. Cancer Ther.* **12**,
602 2378-2388 (2013).
603 43. D. R. Murdoch, R. G. Corey, B. Hoen, M. Miró, V. G. Fowler, A. S. Bayer, A. W. Karchmer, L. Olaison, P. A.
604 Pappas, P. Moreillon, S. T. Chambers, V. H. Chu, V. Falcó, D. J. Holland, P. Jones, J. L. Klein, N. J. Raymond, K.
605 M. Read, M. F. Tripodi, R. Utili, A. Wang, C. W. Woods, C. H. Cabell, Clinical presentation, etiology, and outcome
606 of infective endocarditis in the 21st century The international collaboration on Endocarditis-prospective cohort
607 study, *Arch. Intern. Med.* **169**, 463–473 (2009).
608 44. B. G. Vu, C. S. Stach, K. Kulhankova, W. Salgado-Pabón, A. J. Klingelhutz, P. M. Schlievert, E. Johnson, Ed.
609 Chronic superantigen exposure induces systemic inflammation, elevated bloodstream endotoxin, and abnormal
610 glucose tolerance in rabbits: Possible role in diabetes, *MBio* **6**, e02554-14 (2015).
611 45. J. W. Shupp, M. Jett, C. H. Pontzer, Identification of a transcytosis epitope on staphylococcal enterotoxins,
612 *Infect. Immun.* **70**, 2178–2186 (2002).
613 46. N. W. M. de Jong, T. van der Horst, J. A. G. van Strijp, R. Nijland, Fluorescent reporters for markerless genomic
614 integration in Staphylococcus aureus, *Sci. Rep.* **7**, 43889 (2017).

615 47. D. G. Gibson, L. Young, R.-Y. Chuang, J. C. Venter, C. A. Hutchison III, H. O. Smith, Enzymatic assembly of
616 DNA molecules up to several hundred kilobases, *Nat. Methods* **6**, 343 (2009).
617 48. 23. M. R. Grosser, A. R. Richardson, Method for Preparation and Electroporation in S. aureus and S.
618 epidermidis, *Methods in Molecular Biology*. **1373**, 51–57 (2016).
619 49. 26. J. A. Merriman, P. M. Schlievert, Identification, Purification, and Characterization of Staphylococcal
620 Superantigens, *Methods in Molecular Biology*. **1396**, 19–33 (2016).
621 50. W. Salgado-Pabón, A. Herrera, B. G. Vu, C. S. Stach, J. A. Merriman, A. R. Spaulding, P. M. Schlievert,
622 Staphylococcus aureus β-toxin production is common in strains with the β-toxin gene inactivated by bacteriophage,
623 *J. Infect. Dis.* **210**, 784–792 (2014).
624 51. 30. J. Norrander, T. Kempe, J. Messing, Construction of improved M13 vectors using oligodeoxynucleotide-
625 directed mutagenesis, *Gene*. **26**, 101–106 (1983).
626

627 **Acknowledgements:** We thank the University of Iowa Comparative Pathology Laboratory and
628 University of Iowa Diagnostic Laboratories for histology and serum analysis services. **Funding:**
629 This work was supported by National Institutes of Health (NIH) grant R01AI34692-01 to W.S-P**,**
630 NIH grant 5T32AI007511-23 to P.M.T., and NIH grant T32GM008365 to K.J.K. **Author**
631 **Contributions:** K.J.K. and W.S-P conceptualized and designed experiments, analyzed the data,
632 and wrote the manuscript. K.J.K, P.M.T, A.N.F, K.K, and W.S-P carried out in vivo rabbit
633 experiments. K.N.G-C provided intellectual and technical support on histopathological analysis
634 and gross pathological grading. P.M.T and A.N.F carried out in vitro experiments for the
635 proteomics array and serum analysis. All authors reviewed the manuscript. **Competing**
636 **Interests:** The authors declare no other competing interests. **Data and materials availability:**
637 All the data needed to evaluate the conclusions in this manuscript are present in the manuscript
638 and/or supplementary materials.
639

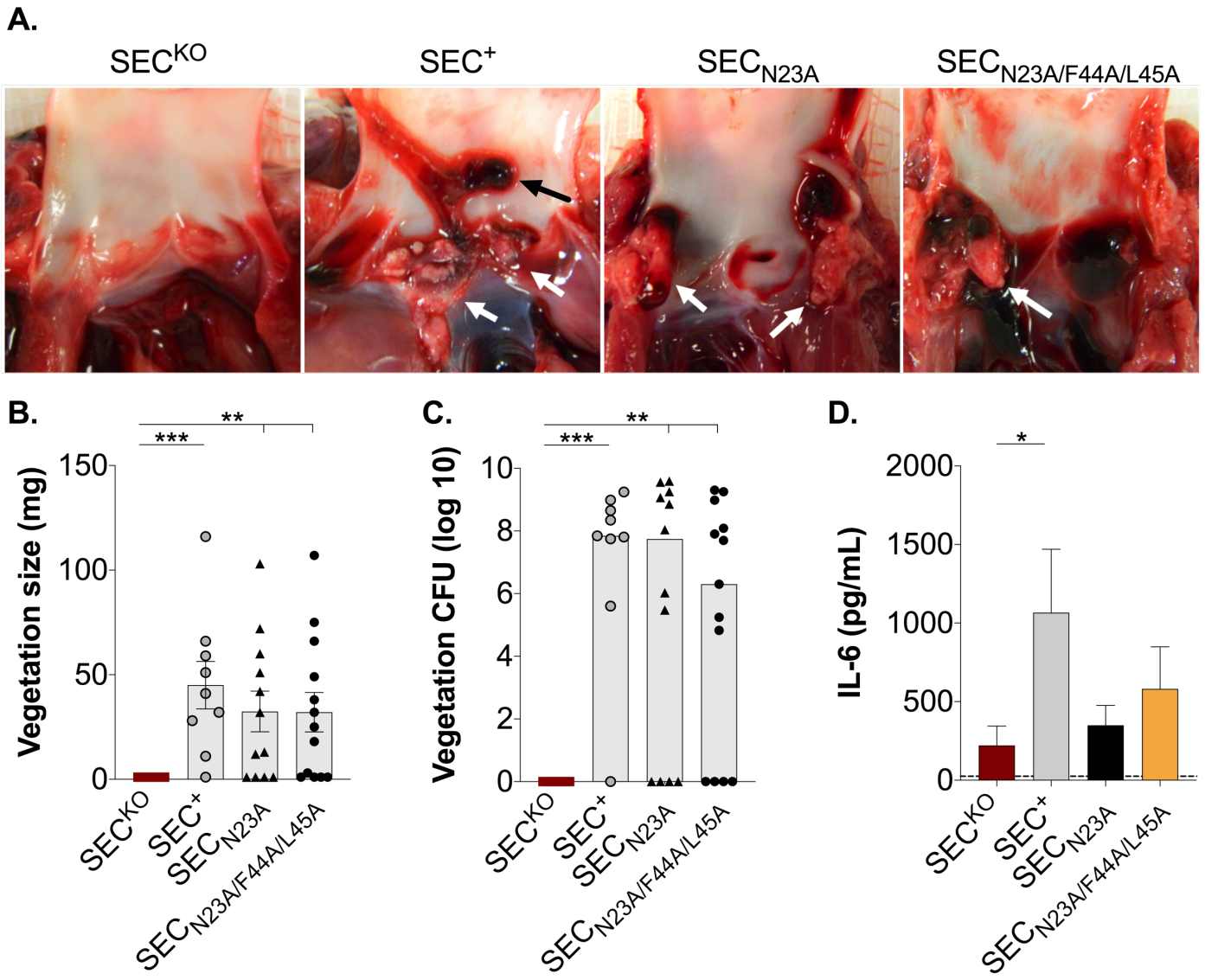

Figure 1. SEC is required for vegetation formation independent of superantigenic activity. (**A**). Representative images of aortic vegetations (white arrow) (black arrow is a post mortem blood clot). (**B**) Total mean weights of vegetations dissected from aortic valves from rabbits infected with indicated strains *S. aureus* SEC^{KO}, SEC^{+}, SEC_{N23A}, $SEC_{N23A/F44A/L45A}$. Error bars are represented by ± SEM. (**C**) Bacterial counts recovered from aortic vegetations from panel B. Bars represent median value. (**D**) Serum analyte levels of interleukin-6 (IL-6) from rabbits 48-96 hpi. Data are represented as mean (± SEM). The dashed line is the average analyte value of all rabbits pre-infection. (**B-D**) Statistical significance was determined by one-way ANOVA with the Holm-Sidak multiple comparison test with each SEC-producing strain compared to SEC^{KO}. (**D**) All groups were tested against pre-

649 infection analyte values and were statistically significant, $p < 0.0001$. (**B**) **, $p = 0.0037$, ***, $p = 0.0004$. (**C**) **, p

650 $= 0.0023$, ***, $p = 0.0003$. (**D**) *, $p \leq 0.0248$. p values ≤ 0.05 are considered statistically significant.

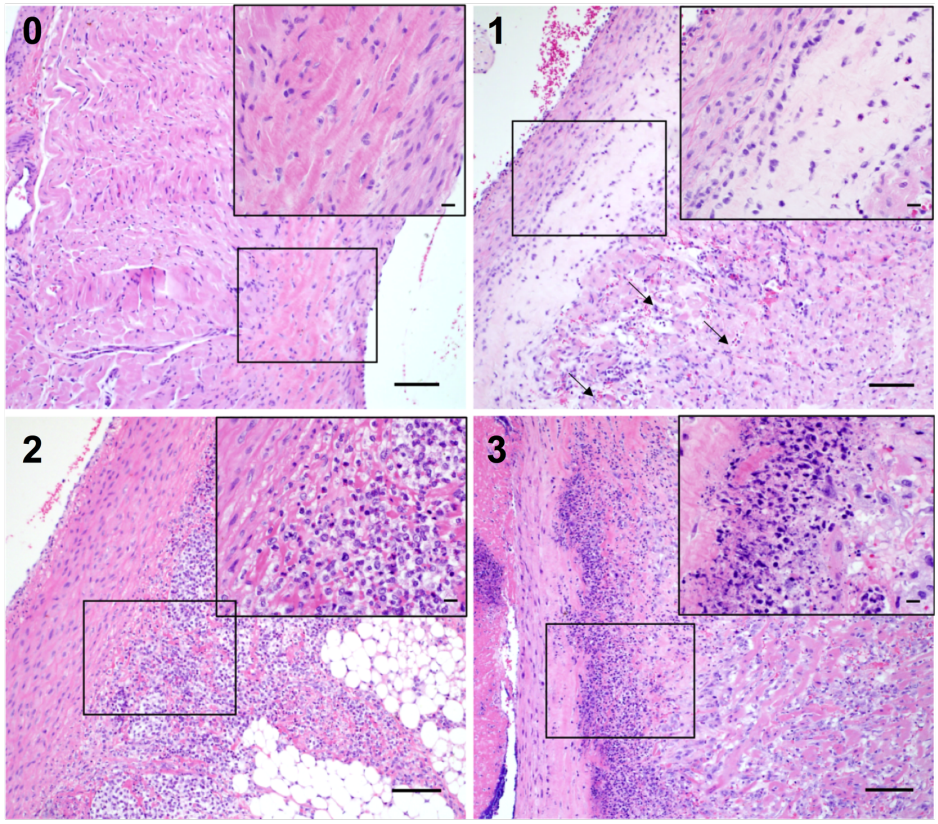

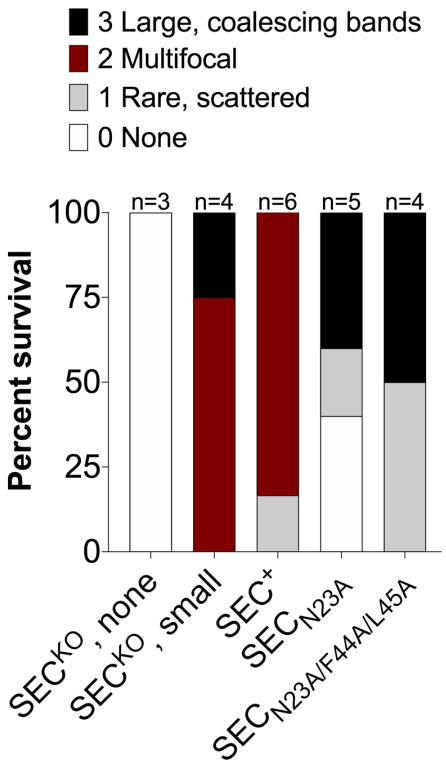

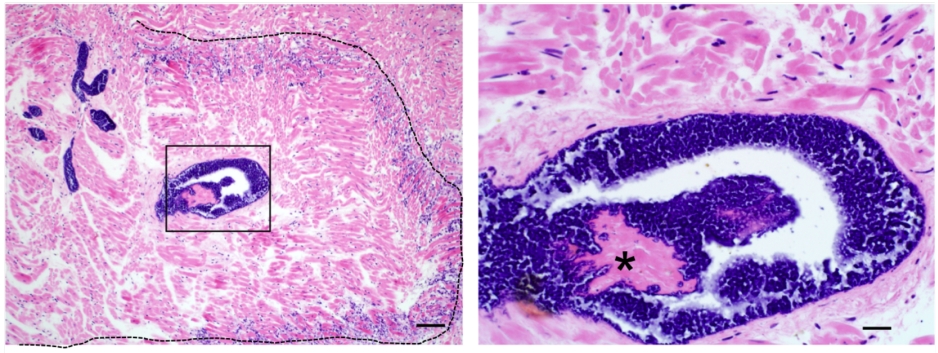

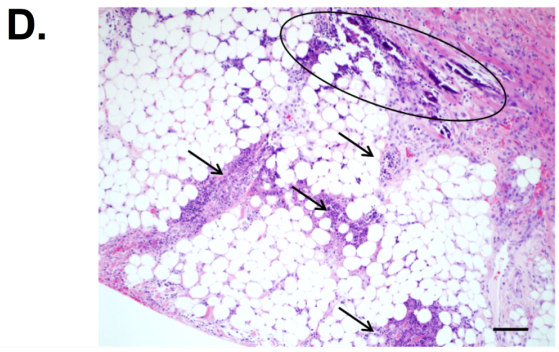

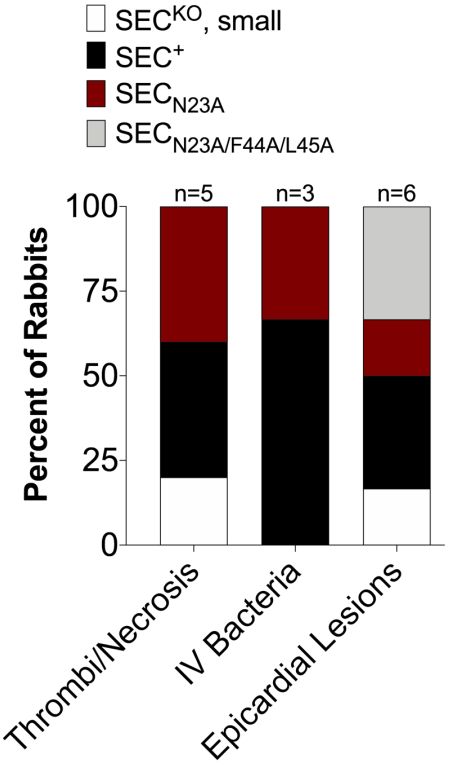

Figure 2. Vegetative lesions present with bacterial infiltration, inflammation, and necrosis. (**A**) Examples of histopathologic assessment of myocardial inflammation during infective endocarditis (Graded 0-3). Inflammation was graded based on the amount of inflammatory cell infiltrate noted within the myocardium. 0 = no inflammation, 1 = multifocal, scattered infiltrate (arrows), 2 = coalescing foci to bands of infiltrate, 3 = wide zones of diffuse infiltrate with necrosis. Bar = 100 µm, inset bar = 20 µm. (**B**) Scoring of myocardial inflammation from HE stained images 48-96 hpi. (**C**) Examples of a fibrinonecrotic focus (dotted outline; note the myocardial necrosis within the outline which is a lighter pink color), (*) a centrally located thrombus and intravascular bacteria (deeply basophilic/blue material). Left bar = 100 µm, right bar = 20 µm. (**D**) Examples of an epicardial lesion with saponification (necrosis) of epicardial fat (arrows) and a locally extensive zone of myocardial mineralization (encircled). Bar = 100 µm. (**E**) Histopathologic scoring the presence or absence of cardiac pathological findings: bacterial thrombi and associated necrosis, intravascular (IV) bacteria, and epicardial fibrin and inflammation.

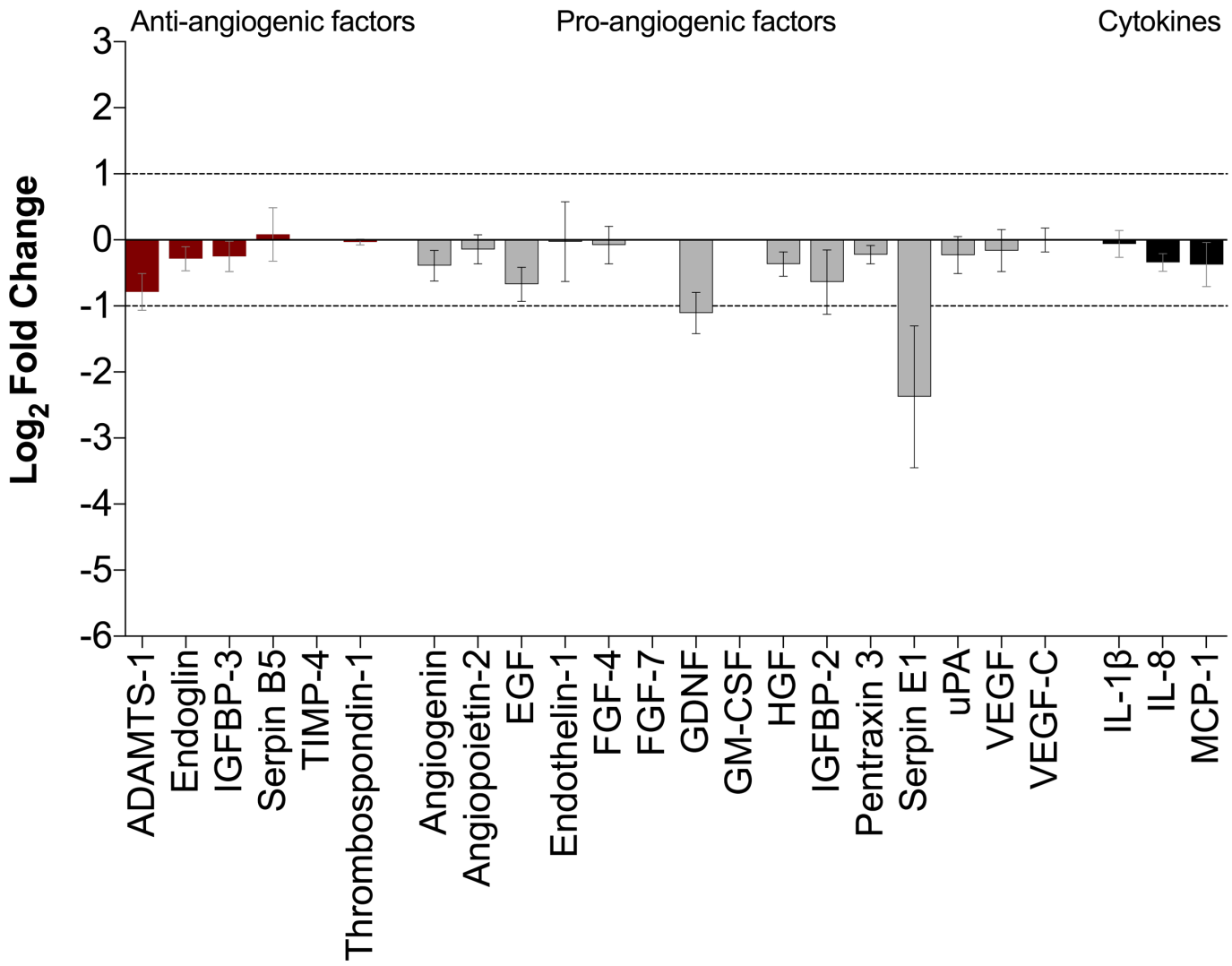

663

664 **Figure 3. SEC elicits anti-angiogenic responses in endothelial cells.** Relative protein abundance of secreted

665 angiogenic factors from iHAECs treated with 20 µg/mL of SEC for 24hrs. Data are represented as mean (± SEM).

666 Log_2 fold change compared to a media control. Dashed line represents threshold for relevant changes set at ± 1.

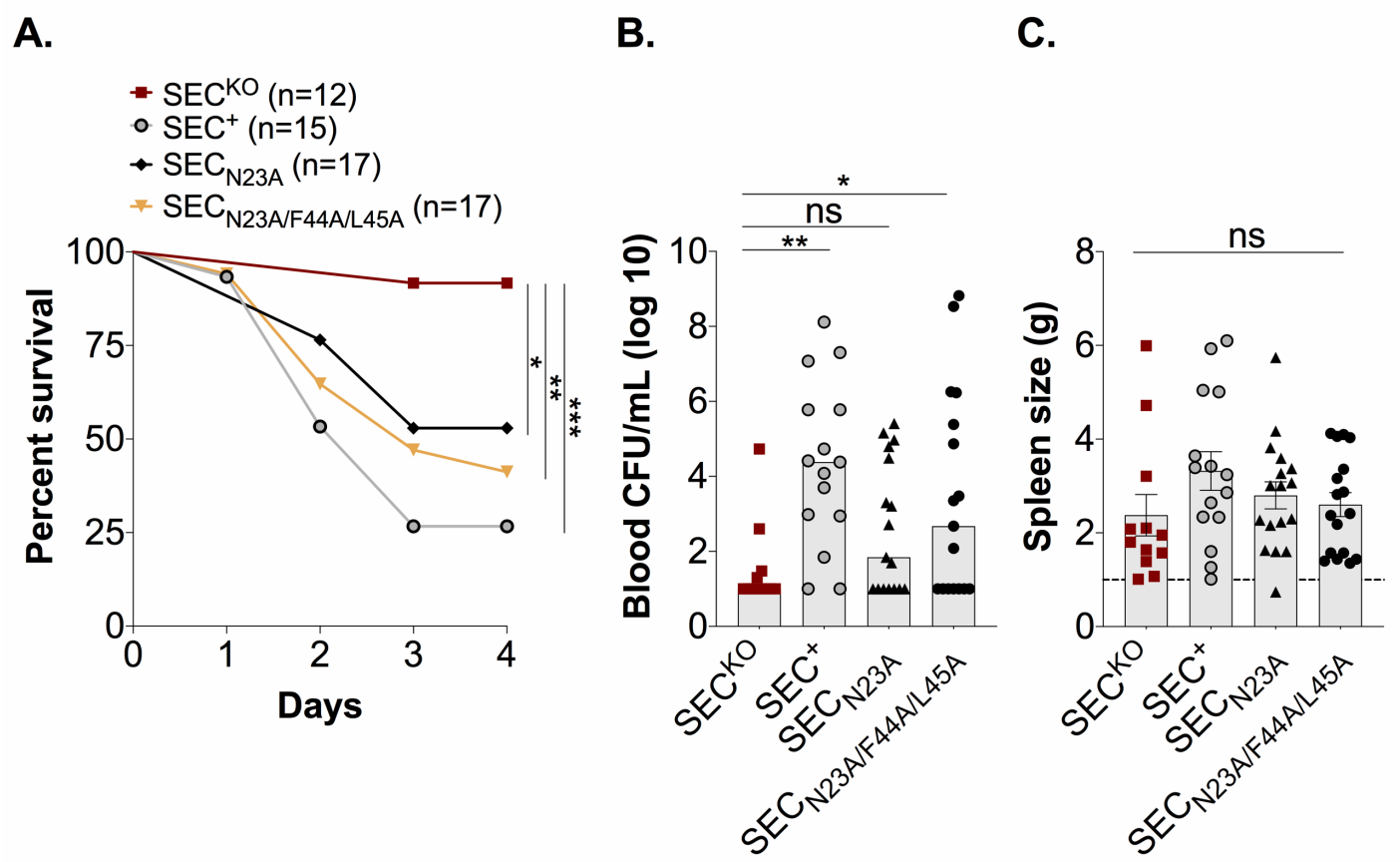

Figure 4. Expression of SEC toxoids leads to systemic infection and lethality. (**A**) Percent survival of rabbits infected intravenously with $2x10^7$-$4x10^7$ CFU of indicated strain measured over 4 days. *, $p = 0.0269$, **, $p = 0.0063$, ***, $p = 0.0007$ log-rank Mantel-Cox Test. (**B**) Bacterial counts per milliliter of blood recovered from rabbits post mortem. Bars represent median value. (**C**) Enlargement of the spleen (splenomegaly) resulting from *S. aureus* infection. Data are represented as mean (± SEM). The dashed line is the average spleen size of uninfected control rabbits. (**B-C**) Statistical significance was determined by one-way ANOVA with the Holm-Sidak multiple comparison test with each SEC-producing strain compared to *S. aureus* SEC^{KO}. (**B**) *, $p = 0.0339$, **, $p = 0.0028$. p values ≤ 0.05 are considered statistically significant.

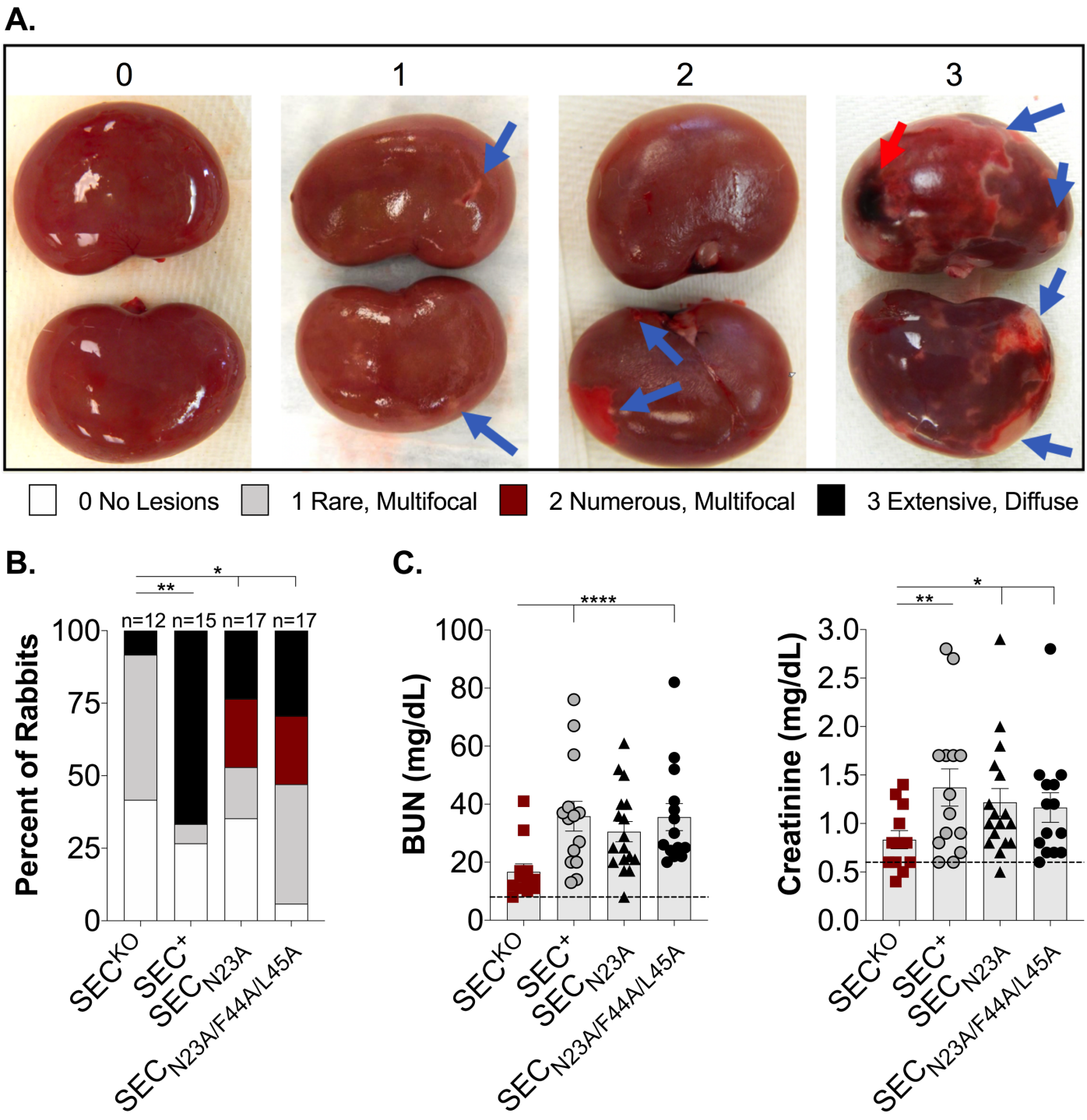

676

677 **Figure 5. SEC toxoids retain ability to cause metastatic infections and renal impairment.** (**A**) Kidney Gross

678 Pathology Grading Scale (Grades 0-3). 0 = no lesions, 1 = rare, small (<4mm) multifocal lesions, 2 = numerous

679 large (>5mm) multifocal lesions, 3 = extensive to coalescing to diffuse lesions. Blue arrows indicate ischemic

680 lesions, red arrow indicates a hemorrhagic lesion. (**B**) Scoring of kidney lesions post mortem. Statistical significance

was determined by the Fisher's exact test comparing categorical pathology grades 0-1 with grades 2-3 between *S. aureus* SEC^{KO} with each SEC-producing strain. (**C**) Serum levels of analytes 48-96 hpi. Data are represented as mean (± SEM). The dashed line is the average analyte values of all rabbits pre-infection. Statistical significance was determined by one-way ANOVA with the Holm-Sidak multiple comparison test. All groups were tested against pre-infection analyte values and were statistically significant, $p < 0.03$. (**B**) *, $p \leq 0.0432$, **, $p = 0.0047$. (**C**) *, $p \leq 0.0397$, **, $p = 0.0046$, ****, $p < 0.0001$. p values ≤ 0.05 are considered statistically significant.

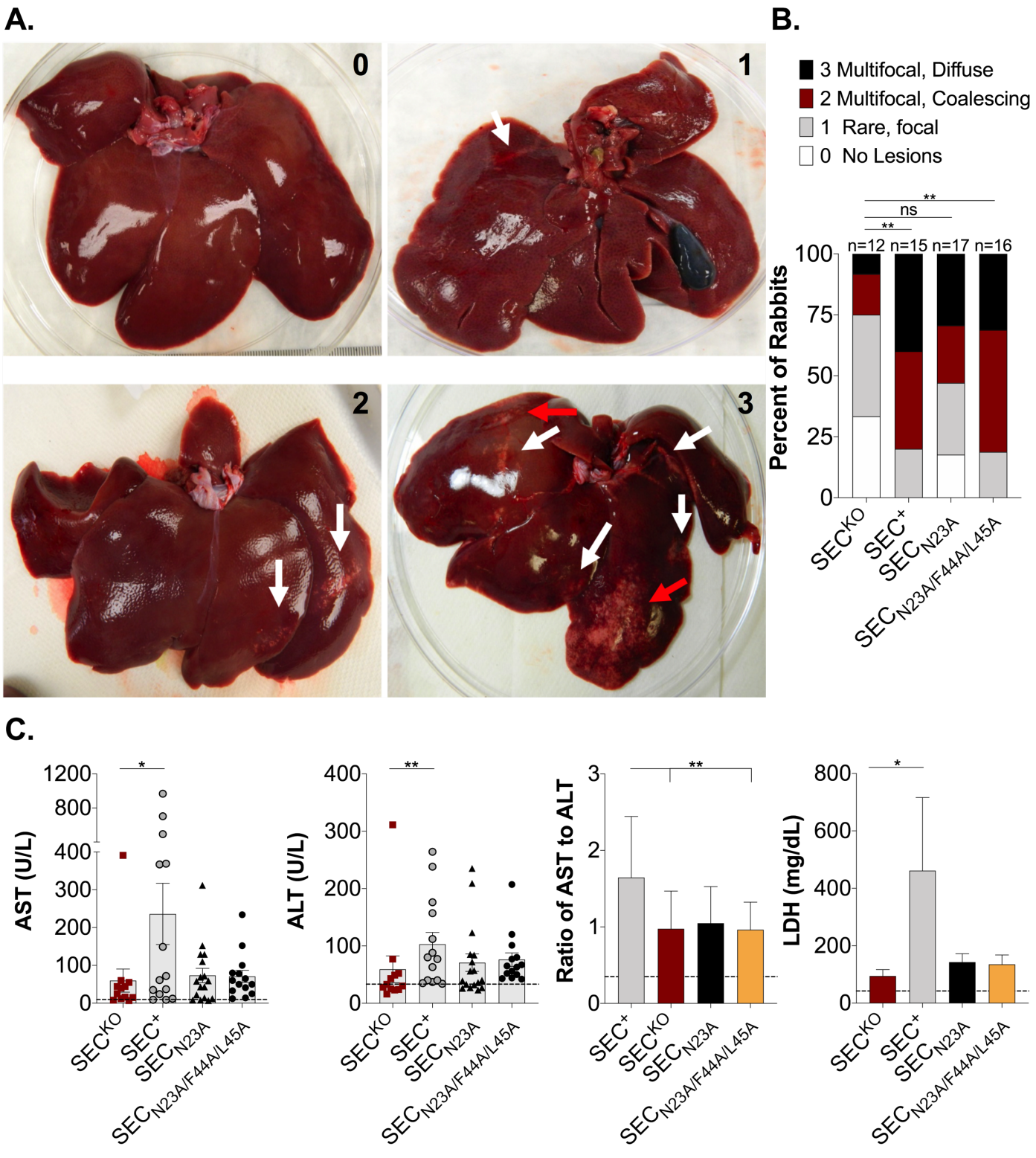

687

688 **Figure 6. Superantigenicity promotes hepatocellular damage.** (**A**) Liver gross pathology grading scale (grades 0-

689 3). 0 = no lesions, 1 = rare, focal streak-shaped lesions, 2 = multifocal to coalescing streak-shaped lesions, 3 =

multifocal streak-shaped extensive to diffuse lesions. White arrows point to streak-shaped ischemic lesions characteristic of grade 1-3, red arrows indicate wide-spread ischemic lesions characteristic of grade 3. (**B**) Scoring of liver pathology post mortem. Statistical significance was determined by the Fisher's exact test comparing categorical pathology grades 0-1 with grades 2-3 between the *S. aureus* SEC^{KO} with each SEC-producing strain. (**C**) Serum levels of analytes 48-96 hpi. Data are represented as mean (± SEM). The dashed line is the average analyte or ratio value of all rabbits pre-infection. Statistical significance was determined by one-way ANOVA with the Holm-Sidak multiple comparison test with each SEC-producing strain compared to SEC^{KO}. All groups were tested against pre-infection analyte values and were statistically significant for AST and LDH with all SEC-producing strains significant for ALT, $p < 0.005$. Statistical significance for AST to ALT ratio was determined by the Fisher's exact test comparing ratio values 0-1.8 to values > 1.8 between the strain SEC^{+} to superantigenic deficient groups (**B**) **, $p \leq 0.0071$. (**C**) *, $p \leq 0.0151$, **, $p \leq 0.0089$. p values ≤ 0.05 are considered statistically significant.